

Geochemical and petrographical evolution of the weathering mantle derived from basalt in Bangam locality (West-Cameroon): implication in the bauxitisation process.

Abstract

A petrographical and geochemical study of the weathering mantle derived from basaltic parent rock (plagioclase, olivine, pyroxene, and zircon) was carried out in Bangam (West-Cameroon). The weathered profile shows a vertical lithology succession of weathered parent rock, isalteritic clayed domain and superficial duricrust (alloterite). The weathering of basalt started by the formation of “ginger bread structure” structure rich in gibbsite, metahalloysite, and kaolinite. The geochemical analysis of major elements indicate that SiO₂ (46% - 1.33%), K₂O (0.84% - 0.01%), Na₂O (3.6% - 0.01%), MnO (0.3% - 0.04%), P₂O₅ (1.9% - 0.38%) and CaO (5% - 0.02%) decrease from the bottom to the surface, however TiO₂ (2.3% - 4.08%) remain constant, while Fe₂O₃ (24.2% - 24.6%) and Al₂O₃ (14.5% - 45.2%) increase. The different weathering indices such as, chemical index of alteration (55% - 99%), index of lateritization (41% - 103.5%) and Ruxton Ratio (0.12 - 3.21) just indicate an evolution of parent rock dominated by an alumina and iron phases under a control of hydrolysis phenomenon as bisialitisation, monosialitisation and allitisation with the formation of minerals of the smectite group, kaolinite group gibbsite and iron oxides group. The fractionation patterns of rare earth elements (REE) show a positive and negative anomaly in Cerium and other rare earth elements, one more, the correlation between major, trace and REE prove a link of different pedological horizons developed on the basalt in redox condition.

Keys words: Basalt, mineral, geochemistry, evolution, bauxite.

1. Introduction

The locality of Bangam and its surroundings are located in zone 32N 636000.651000 and 597500.587000 (Fig. 1). It is subjected to a pseudo-equatorial climate (Dongmo, 1981) with four seasons (Melinguet et al., 1989). The wet savannah is the type of vegetation encountered in Bangam (Letouzey, 1985). On the geological plan, our study area is an integral part of the Cameroon volcanic line (Deruelle, 1982) which crosses the western part of the Cameroonian territory. The formations of the metamorphic basement are represented by mylonitized gneiss with gray or dark color with difficulty showing an alternation of millimetric to centimetric beds composed of quartz, feldspar, garnet-kyanite-biotite or garnet-kyanite-biotite. These rocks were deformed during two tectonic phases (Fozing, 2009). The gneiss with muscovite (orthogneiss) and biotite are also observed, the foliations are very weakly differentiated with pygmatic folds. The plutonic formations are mostly represented by leucocratic granites with a porphyritic granular texture that belongs to the Batié plutonic complex (Talla, 1995) outcropping as a dome syn to late kinematic with a tertiary age (Kwekam, 2005). The volcanic rocks found here are aphyric and porphyric basalts known as “plateau basalt” (Hieronymus, 1972) formed during the second volcanic phase of quaternary (Hieronymus, 1985) with following minerals observed: plagioclase of bytownite-labrador type, olivine and pyroxene. In most cases, these plutonic, volcanic and metamorphic rocks can be transformed in the meteoritic condition in tropical environment to form bauxites. The bauxites duricrust belongs to the family of lateritic soils that occupy around 33% of intertropical zone (Tardy, 1997). They are formed under a dry contrast

tropical climate or wet equatorial climate (Bilong et al., 1992; Aleva, 1994; Temgoua et al., 2002; Bitom et al., 2003 and 2004). In Cameroon, many authors have studied the petrology of lateritic duricrust in Adamaoua (Eno Belinga, 1972), in the West (Momo, 2016) and in the equatorial region (Ndjigui et al., 2008; Nguetnkam et al., 2008; Kamgang et al., 2009; Tsozué et al., 2012; Ndjigui et al., 2013). The study of bauxites in Bangam and its environs have been subjected to some studies scientist research's (Hieronymus, 1973; Sojien, 2007; Momo et al., 2012) on the characterization and cartography of the different bauxites facies, in addition, many geological studies have been done in our research zone (Kwékam, 2005). In a context where the research on bauxites is booming in Cameroon, the previous work on the Bangam Bauxites done by Hieronymus (1972, 1985) and Sojien et al. (2017) were incomplete and their genesis remain unknown, however, no work to date has concentrated on the parent rock evolution, the genesis of bauxites and the transformation of ore body in the alteration mantle. Consequently, the purpose of this work is to identify the exact nature of parent rock and address or show the petrographical and geochemical evolution of alteration coat developed during geological times.

2. Materials and methods

The research was done both on the field and in the laboratory. Firstly, the work on the field consisted of digging trials pits in the form of a toposequence (Fig. 2) in the study area and then, collecting samples immediately from the bottom to the surface following the morphological variations. A morphopedological description was made according to the protocol proposed by Maignien (1968), which consisted of a detailed study of the soil horizons. The samples collected in the alteration coat were sent to the laboratory.

Secondly, in addition to field studies, petrographic analysis were performed on indurated rocks at the Nkolbisson Geology Laboratory of the University of Yaoundé I. Chemical analysis were done on the duricrust and weathered rock at ALS in South-Africa (Alex Steward Laboratory) for major, trace and rare earth elements. Chemical elements identification and quantification were performed by the X-ray fluorescence spectrometry method (ME.ICP 06, ME MS81, OA-GRA05). Spectrometer mass contents are reported as a percentage of oxides (%) for major elements and as part per million (ppm) for trace and rare earth elements.

In addition, three soil weathering indices were inferred from the major element data. They are: the chemical index of alteration ($CIA = [Al_2O_3 / (Al_2O_3 + CaO + Na_2O)] \times 100$) proposed by Nesbitt and Young (1982), the molar ratio SiO_2/Al_2O_3 of Ruxton (1968) and the index of lateritization $[(Al_2O_3 + Fe_2O_3) / (SiO_2 + Al_2O_3 + Fe_2O_3)]$ of Babechuk et al (2014). The geochemical balances to assess the gain and loss of materials was done according the equation $\Psi (\%) = 100 \times [Element (\%)_{horizon} / Element (\%)_{rock} - 1]$ proposed by Malpas et al (2001). A statistical study based on the correlation coefficient of Spearman has been used to treat the different results and the correlation matrix was calculated by Excel software. The REE concentrations were normalized relative to basalt and chondrite (Anders and Grevesse, 1989) to facilitate the comparison of the REE patterns between weathering materials. The (La/Yb) N ratios were calculated to indicate the degree of light rare earth element (LREE) and heavy rare element (HREE) fractionation. Europium (Eu) and Cerium (Ce) anomalies were respectively estimated by comparing the measured concentration of Eu with an expected concentration (Eu*) obtained by interpolation between the normalized values of Sm and Gd and by comparing the measured concentration of Ce with an expected concentration (Ce*) obtained by interpolation between the normalized values of La and Pr as proposed by Taylor and Mc Lennan (1985), the results obtained from the above analyses were carried out to understand the behaviour of chemical elements along the profile.

3. Results

In the Bangam locality, five alteration profiles KY1, KY2, KY3, KY4 and SWa3 (Fig. 2) have been studied according to the toposequence oriented N-S on the southern flank of the Kong-yeni plateau. The alteration profile KY1 has been chosen and illustrated (Fig. 3). It has a depth of 19 m and has three levels of classification and subdivided by pedological horizon from the top of the profile to the parent rock. The geographic coordinates is UTM 32N, 589080 and 640620, at 1680 m of altitude.

3.1. Overview of weathering mantle of KY1

A KY1 weathering mantle has a depth of 19 m and is organized in A_0 , B_{E1} , B_{E2} , B_{E3} , B_{E4} , B_I , C_1 and C_2 horizons. The 0 cm - 10 cm depth consists of the organic horizon A_0 . It is very thin, well leached by a bioturbation phenomenon. The presence of vegetal roots and burrow animals are also noticed in this horizon. The lateritization process is weakly developed and relatively to the high concentration of black soil (7.5G.2/1.5), the transition with the lower eluvial horizon is undulated.

The 10 cm - 300 cm depth consist of the B_{E1} is characterized by a weak presence of very fine grain of materials such as reddish-brown clays (10R.3/3), the high presence of consolidated blocs of duricrust with metric and centimetric sizes. The blocs and boulders are bounded to each other by a fine clay particle. The nodular, massive, pisolitic facies are strongly represented along the profile and their size decreases considerably from the top to the bottom of this horizon. The colour also varies according to the facies and the transition is gradual with the lower horizon by the size of the blocks.

The 300 cm - 400 cm depth consist of the B_{E2} horizon made up of some scattered nodules of reddish (5R.4/9.5), color of centimetric size. The boulder found here has characteristics of pisolitic facies and with irregular sharp edges. The leaching phenomenon is total, with around 80% of blocs having voids full of some mottled clays particles. Mottled clays are sometimes incorporated between blocs and boulders. The brown reddish colour disappears progressively and relatively to the brown grey colour.

The 400 cm - 1000 cm depth comprises different metric blocs and boulders, separated by clay of medium grain of clays. The red colour is dominated (10R.3/3) by other colour that can be observed such as red brown (7.5R.4.5/10). We can also observe a heterogeneity of facies scattered with nodules and pisoliths. The transition with the lower horizon is gradual and the sizes of boulders and blocs decrease progressively toward the bottom.

The 1000cm-1400cm depth consist of the B_{E4} horizon which is characterized by a general dismantling of boulders and we observe the degree of humectation is higher than the upper zone of this profile. The centimetric blocs with polyhedral shapes of duricrust and brown-yellowish clays (10YR.7.5/11) are highly represented. This domain marks the transition between the leaching zone and accumulation zone.

The 1400 cm -1500 cm depth is B_I horizon also called illuviation horizon. It's characterized by very fine grain materials of clay particles, whereby the structure of weathered products haven't been preserved during alteration process. In some places within this horizon, weakly consolidated clays, occur which are relics of the parent rock which are no longer in existence and there is gradual appearance of spotted clays. A little stratification of alumina silicate and ferromagnesian minerals is clearly observed in this part of the profile. Nodules cannot be identified in the clays, however, the colour changes gradually from greyish to whitish.

The 1500 cm - 1650 cm depth is the C₁ horizon or upper isalterite, is a relic of parent rock with a ginger bread structure also called structure in “ginger structure” are clearly identified and indicate the transition between B₁ horizon and C horizon; the limit is progressive toward the bottom with the appearance of greyish colour (7.5GY.4.5/2) and coarse grains particles.

The depth from 1650cm-1850cm is the C₂ is also called lower isalterite. The duricrust is brittle between fingers, has an irregular shape and mainly sandwiched between clay particles. The colour of this horizon is dark-pinkish (5RP.4/12), with ginger bread structure observed in other parts of this horizon can indicate the nature of parent rock. The transition with the next horizon (C₁) is gradual.

At the depth of 1850 cm - 1900 cm, the structure of parent rock is partially conserved and made up of a coarse saprolite. The weathering materials are constituted of compact clays with a greyish colour (7.5GY.4.5/2, the parent rock which presents a weathered cortex that is well developed and a fresh part dark grey with microlitic texture known as basalt. The following description shows that, the alteration coat derived from the basalt rocks under the geochemical and mineralogical transformation.

3.2. Petrographical of sample collected in the weathering mantle

A petrographical study of the sample collected in the weathering zone on thin sections indicates primary minerals such as plagioclases, pyroxenes, olivine and magnetite. Some secondary minerals as kaolinite, hematite, goethite and gibbsite are also observed.

3.2.1. Olivine

Olivine is a ferromagnesian mineral observed in a thin section with an argilosepic matrix (Fig. 4a), it has a brownish colour with many cracks that shows a starting zone of weathering. Pseudomorphosis or iddingsitisation of olivine is proof of the presence of a little fragmented minerals and the gradual domination of iron oxides such as goethite and hematite. The olivine has around 2 mm of size in a thin section and is characterized by a very low pleochroism.

3.2.2. Pyroxene

The pyroxenes (Fig 4b) are easily observable with a size of 2.5 mm and their basal section which presents the two suborthogonals cleavages plans: (110). The cleavages zones might contain a whitish and reddish mineral in natural light. It's mostly associated with clayed minerals characterized by a vosepic structure, the replacement process is gradually observed with the presence of alumina silicate such as kaolinite.

3.2.3. Plagioclases

In thin sections, the plagioclases look like fresh mineral in some sections, and weakly weathered in others (Fig. 4d). It's more over in association with zircon inclusions with an elongated form, of millimeters sizes and preferential orientation. The minerals are also easily identified by their multiple macles. Their size is significantly reduced where the phenomenon of argiliplasmation takes place. We found plagioclases mostly in association with opaque oxides, hydroxides and other alumina silicates and without preferential orientation (insepic).

3.2.4. Hematite /Goethite

Hematite and goethite are represented in thin sections (Fig. 4c) by a reddish and brownish red zone. They are characterized by a low pleochroism and two forms of structural orientation, massive in some sections and insepic in others. They are always found in association between the fissures of primary minerals and which sometimes serve as ferruginous bridges between gibbsite and kaolinite. Hematite and goethite are mostly represented in pisolitic and pseudobréccia facies. Hematite is mostly associated with goethite and appears commonly between primary minerals.

3.2.5. Magnetite

Magnetite appears in thin sections by an irregular shape (Fig. 4b), they have a very dark colour and no pleochroism. It's mostly associated with other Fe-oxides minerals, Al-oxides and with the inclusion of the remains of primary minerals.

3.2.6. Gibbsite

The gibbsite mineral is always colourless in thin sections (Fig. 4b) and there isn't any colour of iron mineral (Delvigne, 1998) and whitish in some sections (Bitom, 1988). It presents as cutanes and appears without orientation (insepic) and always in association with plagioclases and other silicate minerals. Gibbsite is mainly found in the transmineral crack and takes place gradually to the detriment of iron oxides.

3.2.7. Kaolinite

This alumina mineral is strongly observed in a thin section of grey-bluish to whitish colour (Fig. 4b). It's mostly associated with gibbsite and other iron clayed minerals; kaolinite progressively takes the place of some unidentified primary minerals. It is observed here as the grey transition zone of kaolinite which marks the transition from kaolinite to gibbsite. The genesis of kaolinite starts more often in the cracks of primary minerals such as plagioclases and pyroxenes (Moinereau, 1977).

3.3. Geochemical mobilization and redistribution in the weathering mantle

3.3.1. Major and trace elements contents

The major and trace element contents are given in Table 1. According to the table 1 and figure 5, we observe that silica contents decrease significantly from weathered parent rock to the red brown alloterite of the B horizon (SiO_2 : 46 to 1.33%). Inversely, aluminum (Al_2O_3 : 14.35 to 45.2%) and iron (Fe_2O_3 : 24.5 to 38.5%) contents increase relatively toward the surface. Calcium (CaO : 5.0 to 0.02%), sodium (Na_2O : 3.6 to 0.0%), potassium (K_2O : 0.6 to 0.0%), magnesium (MgO : 3.1 to 0.07%) are almost completely leached in the weathering mantle. However, titanium (TiO_2 : 2.3 to 4.08%) and manganese (MnO : 0.3 to 0.04%) remain constant from the weathered rock to the red brown saprolite. Concerning trace elements, we can observe in figure 5 that Cs (0.22- 0.01ppm) and Rb (19.8- 0.3ppm) decrease from the bottom to the surface, Ga (26.2 - 51.1ppm), Nd (34 - 74ppm) and Th (3.69 - 11.85ppm) are slightly constant, however U (0.82 - 4.38ppm), Sn (3 - 4ppm), Sr (474 - 103ppm), V (232-337ppm), Ta (2.2 - 9.4ppm) and Ba (337 - 144ppm) have a zig-zag evolution.

3.3.2. Geochemical evolution of KY1 profile by triangular diagrams and weathering indices

Due to the normalization of the percentage oxides in millication in which the sum of the three elements studied as total value corresponds to the 100 % content, two triangular diagrams $\text{CaO}+\text{Na}_2\text{O}-\text{Al}_2\text{O}_3-\text{K}_2\text{O}$, $\text{SiO}_2-\text{Al}_2\text{O}_3-\text{Fe}_2\text{O}_3$ and molar ratio $\text{SiO}_2/\text{Al}_2\text{O}_3$ have been realized according the table 3. The analysis of the first diagram or diagram of chemical index of alteration (CIA) allow to trace the intensity of alteration in particular, the evolution of feldspath and primary minerals by comparing the departure of Ca, Na, K with the evolution of Al (Fig. 8a). The chemical index of alteration related to weathering intensity, decreases very slightly from the bottom to the surface (Table 3). We observe that Ca, Na, K is mostly leached (impoverishment) in the profile and the major samples are migrated toward the alumina pole (enrichment). In addition, chemical evolution can be also characterized by laterisation process. In this case, the diagram (Fig. 8b) shows that, the parent rock of Bangam profile is not a fresh rock, however, dominated by the kaolinisation at the bottom and the strong laterization on the surface of profile. The IOL values (see table 3) that is controlled by iron indicate both evolution of an alumina phase and iron phase during the laterization process. The molar ratio $\text{SiO}_2/\text{Al}_2\text{O}_3$ or Ruxton Ratio clearly shows the normal evolution of weathering mantle (Table 4). At the bottom of profile or lower isalterite we observe the values between 3.21-3.16, 1.25-1.07 in the lower allotérite and 0.99-0.15 in the upper allotérite.

3.3.2. Major and trace elements balance

The balance calculation of chemical elements of the Bangam alteration profile shows a group of accumulated elements such as Al (21,5%), Ti (2,17%), U (434ppm), Ta (327ppm), Th (260ppm), Zr (174ppm), Ga (120ppm) and Nb (178ppm). The group of exported elements such as Si (- 97.1%), K (- 100%), Na (- 88%), Mn (- 90%), Ba (- 62ppm), Cs (- 100ppm) and Rb (- 100ppm). These elements are strongly leached from the weathered parent rock. The group of zig-zag elements are represented by Fe, Ca, Cr and Sn, which show an enrichment in the isalterite and sometimes are evacuated in the duricrust or upper allotérite. Ba (402 to 14.5ppm), Rb (19.8 to 0.3 ppm), Sr (474 to 103ppm) and Cs (0.22 to 0.00ppm) which are the traces elements in this weathering mantle that decrease, inversely, V (232 to 638ppm), Zr (251 to 689 ppm), followed by Th (3.69 to 11.85 ppm), U (0.82 to 4.38 ppm), Ga (26.2 to 51 ppm) and Sn (3 to 4 ppm) are increasing along the profile. In short, these elements can be classified according to their increasing mobility as follow: $\text{K} > \text{Na} > \text{Si} > \text{Mn} > \text{Ca} > \text{Ba} > \text{Cs} > \text{W} > \text{Cr} > \text{Mg} > \text{P} > \text{Fe} > \text{Rb} > \text{Sn} > \text{Sr} > \text{Al} > \text{Ti} > \text{Ta} > \text{Th} > \text{Zr} > \text{U}$.

3.3.3. Geochemical correlation of Bangam profile

During the bauxitisation process, the chemical elements are redistributed along the profile and are linked by some affinities which permit to correlate them. In this case of the alteration of Bangam profile, we can distinguish positive and negative correlations. Firstly SiO_2 is highly correlated with Sr (0.7), Rb (0.79) and Cs (0.9), CaO with Rb (0.97) and Sr (0.71), Al_2O_3 with Cr (0.725) and Ga (0.891), Na_2O with Cs (0.77), Rb (0.81) Sr (0.8), K_2O with Cs (0.96) and Rb (0.91), La with Pr and La with Ce respectively of 0.95 and 0.93, we can also observed a weak correlation between Al_2O_3 and SiO_2 (0.58), samples are scattered around the graph, contrary to those of REE as La/Pr (0.95) , La/Ce (0.93) and trace elements Sr/Ba (0.85) where samples are nearly concentrated around the graph (Fig 6).

Secondly, MnO is negatively correlated with U (-0.9) and V (-0.8), MgO with U (-0.81) and V (-0.77), Na_2O with Cr (-0.7), Ga (- 0.84), U (-0.8) and V (-0.8), CaO and U (-0.74), K_2O with U (-0.79) and V (-0.94), Al_2O_3 with Rb (-0.84) and SiO_2 (-0.58) , SiO_2 with Cr (-0.8) and U (-0.86).

3.3.4. Rare earth element (RRE) and fractionation

The rare earth elements are mobile during pedogenesis (Nesbitt, 1979; Duddy, 1980; Humphris, 1984; Middelburg et al., 1988; Mc Lennan, 1989). In the Bangam weathered mantle, the results are represented in Table 2: the light rare earth elements (LREE) are more dominant with Ce (27.8ppm - 552ppm), La (40.5ppm - 121ppm) and Nd (11.9ppm - 90.9ppm); the heavy rare earth elements (HREE) which are poorly represented here by Lu (0.18ppm-0.44ppm), Yb (1.27ppm-3.58ppm), and is particularly marked by a high content of Y (6.6ppm-103.5ppm), which is confirmed by the ratio $\sum\text{LREE}/\sum\text{HREE}$ (4.26 - 14.18) in table 2. The chondrite and basalt -normalized (Fig.6) patterns confirm an important enrichment of LREE and an impoverishment of HREE along the profile as others lateritic soils. We also observe accordingly the basalt normalized patterns, a positive anomaly in Ce and Yb, a negative anomaly in Ce, Dy and Tm. In addition, chondrite normalized also shows negative anomaly in Ce, Eu and Ho, a positive anomaly in Ce and Eu. The Eu/Eu* ratio, related to the REE fractionation, varies from 0.38 to 1.13, indicating important fractionation of the REE in various lateritic soil phases, with weak negative Eu anomaly. The Ce/Ce* ratio, included between 0.59 to 1.08 show a positive anomaly of Ce in the coarse saprolite and negative anomaly in the bauxite duricrust. The (La/Yb) N ratio, which ranges from 0.7 to 8.83, also indicates a strong fractionation of the LREE compared to the HREE.

4. Discussion and interpretation

4.1. Chemical evolution in the weathering mantle

The phenomenon of weathering mantle have been studied by many author's such as Trescases (1975) Edou-Minko (1988); Ouangrawa et al. (1996); Ndjigui (2000); Ndjigui et al. (2002); Ekodeck (1984) and the better method to understand weathering mantle in this case of Bangam profile is by using chemical alteration index to appreciate it. The weathering mantle is organized in three levels link by a morphogenesis, according to the texture and structure. The upper domain or alloterite of alteration coat is dominated by a complete transformation of primary minerals and a great blocs of bauxite duricrust, the RR or molar ratio $\text{SiO}_2/\text{Al}_2\text{O}_3$ as indicated in table 3 is very low (Beauvais, 2009). Also a strong CIA translate a high leaching of clay particles in this part of profile and the formation of the gibbsite, goethite, hematite and others iron hydroxides. In the isaltérite, the weathering indices are moderate and less than in the allotérite, it's dominated by mottled clays, this environment indicate an alkaline milieu (Ndjigui et al., 2002) responsible of the formation of kaolinite and others 1/1 minerals such as halloysite and metahalloysite suitable for specific hydrolysis known as monosialtisation (Nahon, 1976 ; Beauvais, 2009; Zobir, 2012). The progression towards the base of profile leads to the primary minerals. In the other hand, the base of profile is also characterized by a low porosity, relics of bedrock, fine grain particles and "ginger bread structural clays. The RR is strong and CIA is low at the base of profile just indicate the presence of 2/1 clays minerals of smectites group Millot (1964), Tardy (1969) such as montmorillonite because of the weak leaching or high contents of Mg, K and Si in this part of the profile (Tematio et al., 2012), these environments are indicative of a highly confined alkaline milieu suitable for hydrolysis known as bisialtisation. The data in the table 4 and figure 3 confirms the hypothesis of an in situ model according to Nahon (1976) and Leprun (1979) where the lithomarge is developed on a basaltic rock. The isaltéritique level which is an intermediate between alloterite and weathered basalt is the domain where the

simultaneous hydrolysis phenomena favorable to the genesis of clays 2/1 and 1/1 completing the uncertain hypothesis of Hieronymus (1972) on the genesis of Bangam bauxites. The antagonism between the RR and CIA as we observe in this case of Bangam KY1 profile is the proof of the chemical elements manifestation in the lateritic zone.

4.2. Petrographical and REE evolution in the weathering mantle

Occurrences of bauxite as a result of the weathering of basalt are reported in Madagascar (Gense, 1970) and in the South-Cameroon (Bilong, 1988) on the syenite weathered mantle. These Bangam bauxite deposits are clearly considered as formed by direct bauxitization process, resulting from initial primary rock. The development of secondary minerals as gibbsite, kaolinite, goethite, hematite and others. Petrographically, these supergene minerals were reported as pseudomorphs after primary minerals such as olivine, pyroxene, plagioclases and magnetite, the replacement was considered isovolumetric as defined by Millot and Bonifas (1955). Therefore, the origin of montmorillonite or some minerals of smectite group was successively investigated in the alteration of plagioclase and pyroxenes respectively by Nguetkam et al. (2003), Craig and Loughnanf (1964) and Loughnanf (1969). Although the first stage of parent minerals weathering generate segregations and spots of iron oxyhydroxides aren't observed in Fig. 2. Iron accumulation is really developed in and can be derive from the alteration of olivine or other ferromagnesian minerals. The first stage of the alteration of plagioclase was classically explained by Bates (1962) and Gense (1970), it can generate a primary gibbsite and metahalloysite present in "ginger bread structure" (greyish section) of first stage of the alteration of basalt. The gain and loss of chemical elements as we observe the mass balance and the distribution translate to the relative and absolute accumulation of major, trace and REE along the Bangam profile according to D'Hoore (1954). KY1 Bangam profile shows that during alteration process, the leaching and mobility of some chemical elements such as Na^+ , Ca^{2+} , K^+ , Mg^{2+} , Mn^{2+} , Si^{4+} are proportional to the degree of weathering (Wronkiewicz & Condie, 1987). These elements are preferably leached (Nesbitt & Young, 1982), whereas Al^{3+} , Fe^{3+} and Ti^{4+} are more often constant in the weathering system (Gresens, 1967; Grant 1986; Potdevin & Caron, 1986; Potdevin & Marquer, 1987). The bauxitisation process is explained by the ternary diagrams of IOL and CIA, which is indicative of a domination by alumina and iron phases (Fig. 8). The transformation of primary minerals as we observe in thin section, shows a progressive change from greyish colour, rich in 2/1 minerals to a whitish-grey, rich in kaolinite and finally whitish, rich in gibbsite. This observation in the thin sections is nothing other than the reflection of the phenomenon that took place in the weathering mantle according to the classification of table 4 based on the molar ratio $\text{SiO}_2/\text{Al}_2\text{O}_3$ or Ruxton ratio adopted by Millot (1964), Tardy (1969) and Beauvais (2009) The antagonism process of lateritic phase, between aluminous minerals such as gibbsite, kaolinite and ferruginous minerals such as goethite and hematite along the weathered zone prove a correlation of chemical elements; an evidence of a genetic link of different horizon (Fig. 6) such as observed by $\text{SiO}_2 - \text{Al}_2\text{O}_3$ and Sr - Ba and others REE isochrons. During pedogenesis, the mobility and structural reorganization of REE involve automatically their fractionation (Duddy, 1980; Humphris, 1984; Middelburg et al., 1988; Mc Lennan, 1989) and consequently the features of the parent rock remain along the Bangam KY1 profile favoured by the circulation of meteorite waters or the pH/Eh of milieu. The Chondrite and basalt -normalized REE indicates a light rare earth enrichment (LREE) relative to heavy rare earths (HREE) due to higher stability of the ligands (sulphates and carbonates) and higher redistribution along the profiles during lateritic alteration Steinberg & Courtois (1976), Topp et al 1984

Trescases et al (1989), Fortin (1986) Marker, De Oliveira (1990); Melfi et al. (1990), Soubies et al. (1990). According to Humphris (1984), the mobilization of the REE during weathering processes results from different factors related to the parent rock mineralogy, specifically the distribution of the REE in the primary bearing minerals, the stability of these minerals during weathering, and their abundance in the parent material. In addition, the low values of (La/Yb) N (0.79-8.83), may be attributed to intense REE fractionation (Moroni et al 2001). The chondrites /samples and basalt/samples normalized patterns (Fig. 7a and 7b) reflect a unique source of samples collected in the alteration zone (Sun & McDonough, 1989) and similar epigenetic transformations for basaltic rocks such as most lateritic profiles Ronov et al. (1967). A light negative anomaly in Ce is due to the oxidation-reduction conditions (Goldberg, 1961) and its incorporation into the ferromanganese-ferric module in the form of ceric oxides or insoluble cerianite Piper (1974); Michard and Renard (1975); Tlig (1982). Sprim (1965) and Piper (1974) also suggest that, negative anomaly in Ce is due of the formation of new minerals especially the montmorillonite. Cerium can occur in the nature as Ce^{3+} in reducing conditions like the majority of lanthanides. Or as Ce^{4+} in oxidizing conditions. If soluble Ce^{3+} is oxidized to Ce^{4+} , it precipitates from solution as very insoluble CeO_2 or according to Braun et al. (1989), Cerium and others lanthanides (Yb, Ho, Dy, Eu...) have a particular fractionation because of their multiple ionic valences. The positive and negative anomaly in the Bangam profile behaviors is due to the moving of phreatic sheet in the alteration weathering which would be responsible for rare earth leaching (Fig. 7a & 7b). In the other hand, alteration coat shows a negative Cerium anomaly may be linked to oxidation of Ce^{3+} to Ce^{4+} or primary Ce^{4+} in residual zircon or sphene minerals because of its oxidation ability, insolubility and stability in lateritic environments (Ndjigui et al., 2008)

5. Conclusion

The weathered profile is dominated by an evolution of alumina and iron phases and the gibbsite observed is the primary and secondary minerals. The mechanism of bauxitisation along the weathering mantle of the Bangam locality shows that the chemical evolution respects the law of lateritization in tropical environment. The bauxitisation process started by the weathering of basalt, characterized by an alternate domain rich in Al_2O_3 and Fe_2O_3 commonly research by the mining company.

The geochemical continuity between the three major levels of alteration confirms that the Bangam bauxites are autochthonous. The bauxitisation process has been strongly influenced by the pH, temperature and the nature of parent rock. The process of bauxitisation has undergone a normal evolution from bisialitisation, monosialitisation to allitisation. In the other words, the different samples are cogenetic, which are formed at the same time, in the same parent rock known as basalt. Since the first tertiary volcanic phase that affected the region of western Cameroon.

References

- Aleva, G. J. J., 1994. Laterites. Concepts, geology, morphology and chemistry. Wageningen: ISRIC. 169p
- Anders .E, Grevesse. N., 1989. Abundances of the elements: meteoritic and solar. *Geochimica and Cosmochimica Acta*, 53 (1) 197 - 214.
- Babechuk, M.G., Widdowson, M., Kamber, B.S., 2014. Quantifying chemical intensity and trace element release of two contrasting profiles. *Decan Traps, India Chemical Geology.*, 365 56 - 75

Bates, T.F., 1962. Halloysite and gibbsite training in Hawaii. Proc. Nat. Conf. Clays and Clays Minerals. 9,307 - 314.

Beauvais, A. 2009. Ferricrete biochemical degradation on the rainforest savannas boundary of Central African Republic. Geoderma. 150, 379 - 388.

Bilong, P., 1988. Genesis and development of ferrallitic soils on alkaline potassium syenite in the forest environment of south-central Cameroon. Comparison with ferrallitic soils developed on basic rocks. Ph.D. dissertation, University of Yaoundé Cameroon.

Bilong, P., Eno. Belinga, S.M., Volkoff, B., 1992. Sequence of evolution of armored landscapes and ferrallitic soils in the tropical forest zone of Central Africa. Place soils with spotted clay horizon. Accounts

Rendus of the Academy of Sciences, Paris, France, 314 (2) 109 - 115.

Bitom, D., Volkoff, B., Abossolo. Angue. M., 2003. Evolution and alteration in situ of a massive iron duricrust in Central Africa. Journal of African Earth Sciences, 37 89 - 101.

Bitom, D., Volkoff, B., Beauvais, A., Seyler, F., Ndjigui, P.D., 2004. Role of lateritic inheritances and groundwater levels in the evolution of landforms and soils in intertropical humid forest zone. Accounts Rendus Geoscience., 336 1161 - 1170.

Biton, D., 1988. Organization and evolution of a ferrallitic cover in tropical humid zone (Cameroon). Genesis and transformation of deep indurated ferruginous whole. Thesis. Univ. Poitiers., 164p. Multigr.

Braun, J.J., Maurice. P, Muller, J.P., Bilong .P, Michard, A., Guillet, B., 1989. Cerium anomalies in lateritic profiles. Geochimica et Cosmochimica Acta 54 781 - 795.

Craig, D.C., Loughnanf, C., 1964. Chemical and mineralogical transformation accompanying the weathering of basic volcanic rocks from New South Wales. Aust. J. Soil Res., 2: 218-234.

Delvigne, J., 1998. Micromorphology of mineral alteration and weathering. The Canadian mineralogist 3, ORSTOM ed., 494p

Deruelle, B., 1982. Volcanic risk in Mount Cameroon. Rev. Geo. Cameroon 3 (1) 33-40.

Dongmo, J. L., 1981. Bamileke dynamisms. Volumes I, the mastery of agrarian space, Yaoundé CEPER,, 424p.

Duddy, R., 1980. Redistribution and fractionation of rare earth and other elements in a weathering profile.

Chem. Geol. 30,363 - 381.

Edou, Minko. A., 1988. Petrology and geochemistry of "stoneline" laterites of the Ovale gold deposit - Application to prospection in humid equatorial zone (Gabon). Th. Doc., Univ. of Poitiers., 147 p.

Ekodeck, G. E., 1984. The alteration of the metamorphic rocks of southern Cameroon and its geotechnical aspects. Th. Doct. State sci. Nat., IRGM, Univ. Scientif. And Medic. From Grenoble I - France., 368 p

Eno, Belinga. S. M., 1972. Alteration of basaltic rocks and process of bauxitization of Adamaoua. State doctoral thesis, Univ. de Paris V ieme. 570 p.

Fortin, P., 1986. Mobilization, fractionation and accumulation of rare earths during lateritic alteration

sandy-clay sediment from the Curitiba Basin (Brazil). Thesis. Same. Sci. of the Earth n010, ENSMP., 186p.

Fozing, E. M., 2009. Study of Amphibolites and Mylonites of the Massif de Fomopéa. Master Thesis, Dschang University, 88p.

Gense, C., 1970. Alteration of basalt in a low-hill of the east coast of Madagascar (morphological unit of this region) Cahier. ORSTOM, ser. Geol. II, 2, 249 - 258.

Goldberg, E.D., 1961. Chemistry in the oceans. In Oceanography (Ed M. Shears). Am. Assoc. Adv. Sci.

Pub., 67-583-597.

Grant, J.A., 1986. The isocon diagram - a simple solution of Gresens' equation for metasomatic alteration. Economic Geology. 1976 - 1982. doi: 10.2113 / gsecongeo.81.8.1976.

Gresens, R.L., 1967. Composition-volume relationships of metasomatism. Chemical Geology, 2: 47-65. 10: 101016 / 0009-2541 (67) 90004-6.

Humphris, S.E., 1984. The mobility of the rare earth elements in the crust. In Rare Earth Element Geochemistry (P. Henderson ed.) Elsevier, Chap. 9, 317-340.

Hieronymus, B., .1985. Study of the alteration of eruptive rocks of western Cameroon. Unpublished Doctorate of Sciences. Thesis university Paris Vlieme.

Hiéronymus, B., 1973. Mineralogical and geochemical study of bauxite formations in western Cameroon. ORSTOM Collection, 77 - 112.

Hieronymus, B., 1973. Lateritic bauxites and bauxites: case of the forest-savanna contact of South-East Cameroon, state thesis, University of Yaoundé-1, 208p.

Kwékam, M., 2005. Genesis and evolution of the calc-alkaline granitoids during pan-African tectonics: the case of the syn-late to late-tectonic massifs of western Cameroon (Dschang and Kékem region). State Thesis, University of Yaoundé I, 175 p.

Kamgang, K. B. V, Onana, V. L., Ndome, E.P., Parisot, J.C., Ekodeck. G. E., 2009. Behavior REE and mass balance calculations in a laterite profile of chlorite schists in South Cameroon. Chemie der Erde-Geochemistry, 69 61-73.

Leprun, J.C., 1979. The ferruginous cuirasses of the crystalline countries of dry West Africa. Genesis-processing-degradation. Same. Geological Sci, 58. 224p

Letouzey, R., 1985. Phytogeographic study of Cameroon. Edition .p. Lechevelier, 511p.

Loughnan, J.C., 1969. Chemical weathering of the silicate minerals. Am. Elsevier Publ. Comp. l'nc. New York., 146 p.

Michard, G. Renard D., 1975. Possibilités d'entraînement du cobalt, du plomb et du cérium dans les nodules de manganèse par oxydation. C. R. Acad. Sc. Paris 280, 1761-1764.

Moroni, M., Girardi V.A.V., Ferrario, A., 2001. The Serra Pelada Au-PGE deposit, Serra dos Carajas (Para State, Brazil): geological and geochemical indications for a composite mineralising process. Mineral Deposita, 36, 768 - 785.

Melfi, A. J., Figueiredo, A. M., Kronberg, B.1., Dohert, W. D., Marques, L. S., 1990. REE mobilities during incipient weathering of volcanic rocks of the Parana Basin, Brazil. (Abs.). Chem. Geol.

- 84., 375 - 376.
- Marker, A. De Oliveira. J. J., 1990. The formation of rare earth element scavenger minerals in weathering products derived from alkaline rocks in SE-bahia, Brazil. (Abs.). *Chem. Geol.*, 84, 373 - 374.
- Millot, G., 1964. *Géologie des argiles*. Masson et Cie, éd., Paris, 499 p.
- Mc Lennan, S. M., 1989. Rare earth elements in sedimentary rocks: influence of provenance and sedimentary processes. In *Geochemistry and mineralogy of rare earth elements*. (éd. Lipin B. R. & McKay G. A.), *Reviews in mineralogy* 21, 169 - 196.
- Middelburg, J. J., Van Der Weijden, C. H., Woittiez, J. R. W., 1988. Chemical processes affecting the mobility of major, minor and trace elements during weathering of granitic rocks. *Chem. Geol.*, 68, 253 - 273.
- Moinereau, J., 1977. *Altération des roches, formation et évolution des sols sur basalte sous climat tempéré humide*. Thèse de Doct. d'Etat. Univ. des Sci. et Tech. du Languedoc, 197P.
- Malpas, J., Duzgorec-Aydin, N. S., Aydin, A., 2001. Behaviour of chemical elements during weathering of pyroclastic rocks, Hong-Kong. *Environment International*, 26, 359 - 368.
- Maignien, R., 1968. *Manuel de prospection pédologique*. Doc ORSTOM. Manuel sur les routes dans les zones tropicales et désertiques. Tome 2. étude technique de construction, 244 - 277. BCEOM-CEBTP, 1991.
- Melingui, A., Gwanfogbe, M., Ngoughia, J., 1989. *Géographie du Cameroun*. Edition CEPER. Yaounde, 119p
- Momo, N.M., Tematio, P., Yemefack, M., 2012. Multi-Scale Organization of the Doumbouo-Fokoué Bauxites Ore Deposits (West Cameroon): Implication to the landscape Lowering. *Open journal of geology* 14 - 24.
- Momo, N. M., 2016. *Les surfaces latéritiques cuirassées du plateau Bamiléké (Ouest-Cameroun): cartographie du potentiel bauxitique, pétrologie, contexte morpho-tectonique et dynamique du paysage*. Thèse de doctorat/PhD. Univ. Dschang, 223p.
- Millot, G., Bonifas, M., 1955. Transformations isovolumétriques dans les phénomènes de latéritisation et de bauxitisation. *Bull. Serv. Carte Géol. Alsace. Lorraine* 8, 3 - 10.
- Ndjigui, P.D., 2000. *Métallologie de la serpentinite de Kondong I et de son manteau d'altération dans le Sud-Est du Cameroun : pétrographie, minéralogie et géochimie*. Th. Doc. 3e cycle, Univ. Yaoundé I, 170 p.
- Ndjigui, P.D., Bitom, D., Bilong, P., Colin, F., Ali, H. N., 2002. Correlation between Metallic Oxides (Fe₂O₃, Cr₂O₃, NiO) Platinum and Palladium in the Laterites from Southeast Cameroon (Central Africa): Perspectives of Platinoids Survey in Weathering Mantles, 9th international platinum symposium, Abs. Duke university.
- Ndjigui, P. D., Bilong, P., Bitom, D., Dia, A., 2008. Mobilization and redistribution of major and trace elements in two weathering profiles developed on serpentinites in the Lomie' ultramafic complex, South-East Cameroon, *Journal of African Earth Sciences*, 50, 305 - 328.
- Ndjigui, P. D., Badinane, M. F. B., Nyeck, B., Nandjip, H. P. K., Bilong, P., 2013. Mineralogical and

geochemical features of the coarse saprolite developed on orthogneiss in the SW of Yaoundé, South Cameroon, *Journal of African Earth Sciences*, 79, 125 - 142.

Nguetnkam, J. P., Bitom, D., Yongue, R., Bilong, P., Belinga, E.S.M., Volkoff, B., 2003. Etude pétrologie, minéralogique et géochimique d'une toposéquence de sols développés sur granite dans le plateau forestier Sud-Camerounais. *Sciences, Technique et Développement*, 10, 35 - 43.

Nguetnkam, J. P., Kamga, R., Villiéras, F., Ekodeck. G. E., Yvon, J., 2008. Altération différentielle du granite en zone tropicale. Exemple de deux séquences étudiées au Cameroun (Afrique Centrale). *Comptes Rendus Géoscience*, 340, 451 - 461.

Nesbitt, H.W., Young, G.M., 1982. Early Proterozoic climates and plate motions inferred from major element chemistry of lutites. *Nature*, 199, 715 - 717.

Nesbitt, H.W., 1979. Mobility and fractionation of rare earth elements during weathering of granodiorite, *Nature*, 279: 206-210. doi:10.1038/279206a0.

Nahon, D., 1976. Cuirasses ferrugineuses et encroutements calcaires au Sénégal oriental et en Mauritanie. Systèmes évolutifs: géochimie, structures, relais et coexistence. *Mém. Sci. Géol.*, 44, 232 p., 12 pl. h.t.

Ouangrawa, M., Trescases, J.-J., Ambrosi, J.P., 1996. Evolution des oxydes de fer au cours de l'altération de roches ultrabasiques de Nouvelle Calédonie : *C.R. Acad. Paris*, 323, Ila, 243 - 249.

Piper, D. Z., 1974. Rare earth elements in ferromanganese nodules and other marine phases. *Geochim. Cosmochim. Acta* 29, 1007 - 1022.

Potdevin, J.L., Caron, J.M., 1986. Transferts de matière et déformation synmétamorphique pli. I: Structures et bilans de matière. *Bulletin de Minéralogie*. 109 (4) 395-410.

Potdevin, J.L., Marquer, D., 1987. Méthodes de quantification des transferts de matière fluides dans les roches métamorphiques déformées. *Geodynamica Acta* 1 (3): 193-206.

Ronov, A.B., Balashov, Y.A., Migdisov. A. A., 1967. Geochemistry of the rare earths in the sedimentary cycle. *Geochem. Inti*, 4, 1 - 17.

Ruxton, B.P., 1968. Measures of the degree of chemical weathering of rocks. *Journal of Geology*, 76.

Soubies, F., Melfi, A.J., Autefage, F., 1990. Geochemical behavior of rare earth elements in aiterites of phosphate and titanium ore deposits in Tapira (Minas Gerais, Brazil): the importance of phosphates. *Chem. Geol.* 84, 376 - 377.

Steinberg, M., Courtois, C., 1976. The behavior of rare earths during alteration and its consequences. *Bull. Soc. Geol. France* 1, 13 - 20.

Sojien, M. T., 2007. Petrographic, Mineralogical and Geochemical Study of Bauxite Formations of Bangam in the Western Highlands of Cameroon. MSc dissertation, Dschang University, Dschang, p. 77.

Sojien, T. M, Mamdem T. E. L., Wouatong, A. S. L, Bitom, D, L., 2017. Mineralogical and Geochemical Distribution Study of Bauxites in the Locality of Bangam and Surroundings (West Cameroon). *Earth Science Research*; 7 (1) 117 - 131.

Sun, S., Mc Donough, W.F., 1989. Chemical and isotopic systematics of oceanic basalts; implications

for

mantle composition and processes. In: *Magmatism in the Ocean Basins*. (Saunders, A.D. & Norry, M.J.Eds.). Geological Society of London, London, United Kingdom, 313 - 345.

Talla, V., 1995. The pan-African granitic massif of Batié (West Cameroon): petrological petrology-geochemistry. Doctorate thesis 3rd cycle. Univ. from Yaounde, 144p.

Tardy, Y., 1969. Geochemistry of alterations. Study of arenas and waters of some crystalline massifs of Europe and Africa. State Doctorate Thesis, Strasbourg University, Mémoires du Service de la Carte géologique. Alsace-Lorraine, No. 31, 199 p.

Tardy, Y., 1997. Petrology of laterites and tropical soils. Balkema, Amsterdam, the Netherlands, 459p.

Taylor, S.R., Mc Lennan, S.M., 1985. *The Continental Crust: its Composition and Evolution*. Blackwell, Oxford, 321p.

Temgoua, E., Bitom, D., Bilong, P., Lucas, Y., Pfeifer, HR, 2002. Dismantling of old battleship landscapes in the tropical forest zone of Central Africa, formation of current ferruginous accumulations at the bottom of the slopes. *Accounts Geoscience*. 334, 537-543.

Tematio, P., Kombou, N.A., Kengni, L., Nguetnkam, J.P., Kamgang, K.V., 2012. Mineral and geochemical characterization of the weathering mantle derived from norites in Kekem (West-Cameroon): evaluation of the related mineralization. *International Research Journal of Geology and Mining (irjgm)*, (2276-6618) 2 (8) 230-242.

Tlig, S., 1982. Distribution of rare earths in sediment fractions and associated Fe and Mn nodules in Indian Ocean. *Mar. Geol.*, 50, 257-274.

Topp, S. E., Salbu, B., Roaldset, E., Jorgensen P., 1984. Vertical distribution of trace elements in laterite soil (Suriname). *Chem. Geol.* 47, 159 - 174.

Trescases, J. J., Fortin, P., Melfi, A., Nahon, D., 1986. Rare earth elements accumulation in lateritic weathering of Pliocene sediments, Curitiba basin (Brazil). In *Proceeding of the International Meeting Geochemistry of the Earth Surface and Process of Mineral Formation*. Grenade, 260 - 271.

Trescases, J.J., 1975. L'évolution géochimique supergenes des roches ultrabasiques en zone tropicale. Formation des gisements nickélicifères de Nouvelle-Calédonie : Mém. ORSTOM. 78, 259 p.

Tsozué, D., Bitom, D., Yongue F. R., 2012. Morphology, mineralogy and geochemistry of a lateritic soil sequence developed on micaschist in the Abong-Mbang region, southeast Cameroon, *south African journal of geology*, 115 (1) 103 - 116.

Wronkiewicz, D.J., Condie, K.C., 1987. Geochemistry of Archean shales from the Witwatersrand Supergroup, South Africa: source-area weathering and provenance. *Geochimica et Cosmochimica Acta*, 51 2401 - 2416. doi:10.1016/0016-7037(87)90293-6.

Zobir, H. S., 2012. Impact de l'altération sur le bilan chimique des diatexites du Massif de l'Edough (Annaba, NE Algérien) *Estudios Geológicos.*, 68 (2) 203 - 215 Issn: 0367-0449 doi:10.3989/egeol.40612.158.

Table 1 Geochemistry of traces, majors elements.

Horizon	PR	C1	C2	BI	BI	BE	BE	BE	BE	BE	
Sample	P1	P2	P3	P4	P5	P6	P7	P8	P9	P10	
Colour	G	Gy	Gy	Wp	Rb	R	Br	Br	Br	Wy	
Depth(m)	19.00	18.50	17.00	15.00	11.50	8.00	6.00	2.00	1.00	0.30	
lithology	B	WB	WB	Fs	Sc	Nd	Pd	Md	Md	Md	
Oxides(%) DL											
SiO₂	0.01	46	42.5	44.9	29.3	21.2	28.2	29.9	6.38	4.5	1.33
Al₂O₃	0.01	14.35	17.2	14.23	23.5	40.7	35.7	30.2	35.2	30.2	45.2
Fe₂O₃	0.01	24.5	25.6	21.3	25.4	10.9	38.56	18.1	32.6	38.5	24.6
CaO	0.01	5	2	8.2	0.03	0.06	0.02	0.05	0.02	0.02	0.02
MgO	0.01	3.1	2.16	4.29	0.19	0.11	0.05	0.16	0.1	0.08	0.07
Na₂O	0.01	0.98	3.6	2.87	<0.01	<0.01	0.01	0.01	<0.01	<0.01	<0.01
K₂O	0.01	0.6	0.84	0.45	0.02	0.02	0.03	0.01	0.01	<0.01	<0.01
TiO₂	0.01	2.3	7.3	5.01	7.1	5.56	4.5	5.78	5.09	4.02	4.08
MnO	0.01	0.3	0.25	0.2	0.1	0.03	0.05	0.08	0.05	0.05	0.04
P₂O₅	0.01	1.9	2.3	1.23	0.35	0.46	0.93	0.4	0.44	0.7	0.38
Trace elements (ppm)											
Ba	0.5	337	297	287	14.5	402	126	335	125	121	144.5
Cs	0.01	0.22	0.26	0.12	0.01	<0.01	0.01	0.03	<0.01	<0.01	<0.01
Ga	0.1	26.2	25.4	36.5	42	59.2	55.5	41.5	57.9	48.6	51.1
Nb	0.2	34.2	25.2	62.3	41.7	59.9	35.6	43.3	95.4	49	74.5
Rb	0.2	19.8	17.8	21.3	0.6	0.6	0.32	0.6	0.5	0.3	0.3
Sn	1	3	3.5	7	3	4	2	3	6	5	4
Sr	0.1	474	464	424	6	418	145	273	91.8	79.7	103
Th	0.05	3.69	4	8.23	4.26	7.98	5	6.34	13.3	7.59	11.85
U	0.05	0.82	0.9	0.85	2.27	2.79	4.23	1.97	3.12	3.83	4.38
Zr	2	251	623	297	340	490	332	345	689	391	543
V	5	232	145	330	580	603	652	482	638	603	337
Ta	1	2.2	3.9	3.2	2.5	3.4	2	2.6	5.2	2.5	9.4
LOI		4.1	4.2	3.2	13.9		17.23	14.55	20.2	19.9	25.5
Total		103.6	104.2	103.25	99.91	99.76	99.54	99.3	100.13	98	101.27

G=grey; Gw=whitish grey; Gy=Yellowish grey; Wy=Yellowish-white; Wp=Whitish-pink; Rb=red brown; R=redish; Br=brown red; Md=massive duricrust; Pd=Pisolitic duricrust; Nd=nodular duricrust; B=basalt; Wb=weathered basalt; Cs=coarse saprolite; Fs=Fine saprolite; Sc=Spotted clays; DI=detection limit.

Table 2 Rare earth element and fractionation

Horizon	PR	C1	C2	BI	BI	BE	BE	BE	BE	BE	
Sample	P1	P2	P3	P5	P7	P8	P9	P11	P12	P13	
Colour	G	Gy	Gy	Wp	Rb	R	Br	Br	Br	Wy	
Depth(m)	19.00	18.50	17.00	15.00	11.50	8.00	6.00	2.00	1.00	0.30	
lithology	B	WB	WB	Fs	Sc	Nd	Pd	Md	Md	Md	
RRE(ppm)	DI										
La	0.5	40.5	100	41	13.6	100.5	121	278	79	89.8	65.1
Ce	0.5	87.7	83.7	86.3	27.8	186	171	552	133.5	162.5	123.5
Pr	0.03	12.35	13	14.26	3.12	22.7	23.66	69.4	18.1	19.65	1.2
Nd	0.1	55.7	18	24	11.9	90.9	75.6	253	75.2	75.7	61.1
Sm	0.03	13.25	12.5	11.5	2.59	20.2	23	50.5	15.5	15.7	13.05
Eu	0.03	3.45	1.35	2.37	0.6	4.95	4	12.1	3.49	3.32	3.52
Gd	0.05	12.05	13	11	1.79	17.7	13.5	30.2	12.45	12.1	11
Tb	0.01	1.8	1.5	1.6	0.33	2.78	1.62	4.06	1.68	1.4	1.51
Dy	0.05	9.03	11	5	1.81	18.15	8.23	18.8	8.48	8.74	7.19
Ho	0.01	1.67	2.4	2	0.35	4.27	1.3	2.48	1.29	1.28	1.08
Er	0.03	4.39	3.3	4.7	1.04	10.8	2.6	4.82	2.82	2.66	2.31
Tm	0.01	0.58	0.39	0.49	0.16	0.93	0.36	0.46	0.37	0.31	0.22
Yb	0.03	3	2.35	4.3	1.27	3.58	1.75	2.33	2.16	1.76	1.36
Lu	0.01	0.44	0.24	0.44	0.18	0.35	0.25	0.24	0.32	0.26	0.19
Hf	0.2	6.5	15	17.2	8.4	11.6	8.2	8.6	15.9	9.4	12.8
Y	0.5	41	36	45	6.6	103.5	29.9	35	23.9	21.5	19.5
RRE index											
Σ REE	245.91	262.73	208.96	66.54	483.81	447.87	1278.39	354.36	395.52	306.33	
LREE/HREE	4.264	5.75	4.79	6.42	5.28	10.66	14.18	7.79	9.42	8.19	
(La/Yb)N	1	3.15	0.7	0.79	2.07	5.12	8.83	2.7	3.77	3.54	
Eu/Eu*	1	0.38	0.77	1.02	0.95	0.83	1.13	0.92	0.88	1.07	
Ce/Ce*	1	0.59	0.91	1.08	0.99	0.81	1.01	0.9	0.98	1	

G=grey; Gw=whitish grey; Gy=Yellowish grey; Wy=Yellowish-white; Wp=Whitish-pink; Rb=red brown; R=redish; Br=brown red; Md=massive duricrust; Pd=Pisolitic duricrust; Nd=nodular duricrust. DI=detection limit

Table 3 Chemicals index of alteration of KY1 profile.

Chemicals index	Samples collected along of KY1 profile									
	P1	P2	P3	P4	P5	P6	P7	P8	P9	P10
CIA (%)	55	57	68	72	99	99	99	99	99	99
IOL (%)	41	44	46	50	62	65	70	91	98	103
RR	3.21	3.16	1.25	1.07	0.52	0.99	0.18	0.12	0.18	0.15

Table 4 Evolution of hydrolysis phenomenon of profile KY1.

Pedological					
level	Samples	Lithology	SiO ₂ /Al ₂ O ₃	Hydrolysis process	Minerals
alloterite	P10	Md	0.15	allitisation	Gibbsite, Goethite, Hematite and other Fe-oxides
	P9	Md	0.18		
	P8	Pd	0.12		
	p7	Pd	0.18		
	P6	Nd	0.99		
	P5	Sc	0.52		
isalterite	P4	Fs	1.07	monosiallisation	Halloysite/Metahalloyiste Kaolinite,
	P3	Cs	1.25		
Weathered Parent rock	P2	Bw	3.16	bisialitisation	Smectite (montmorillonite)
	P1	B	3.21		

B=basalt; **Bw**=weathered basalt; **Cs**=coarse saprolite; **Fs**=Fine saprolite; **Sc**=Spotted clays; **Md**=massive duricrust; **Pd**=Pisolitic duricrust; **Nd**=nodular duricrust brown.

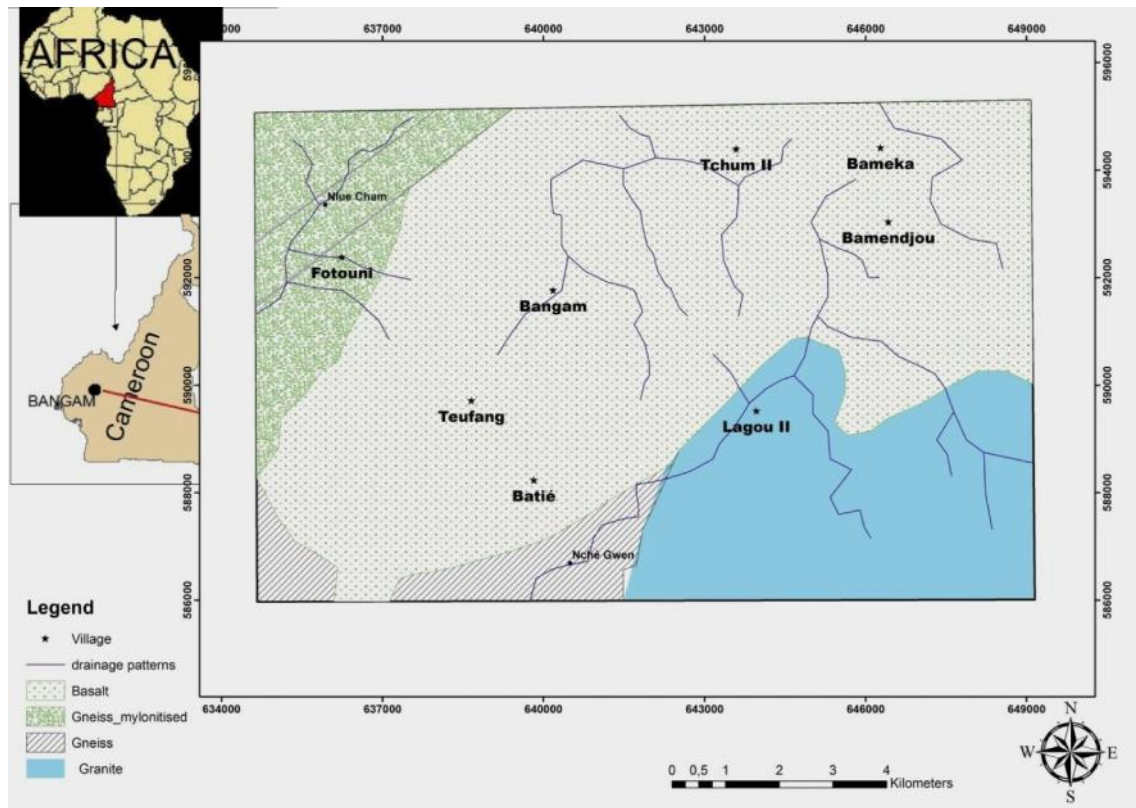


Fig. 1. Location and geological Map of Bangam in the west-Cameroon region

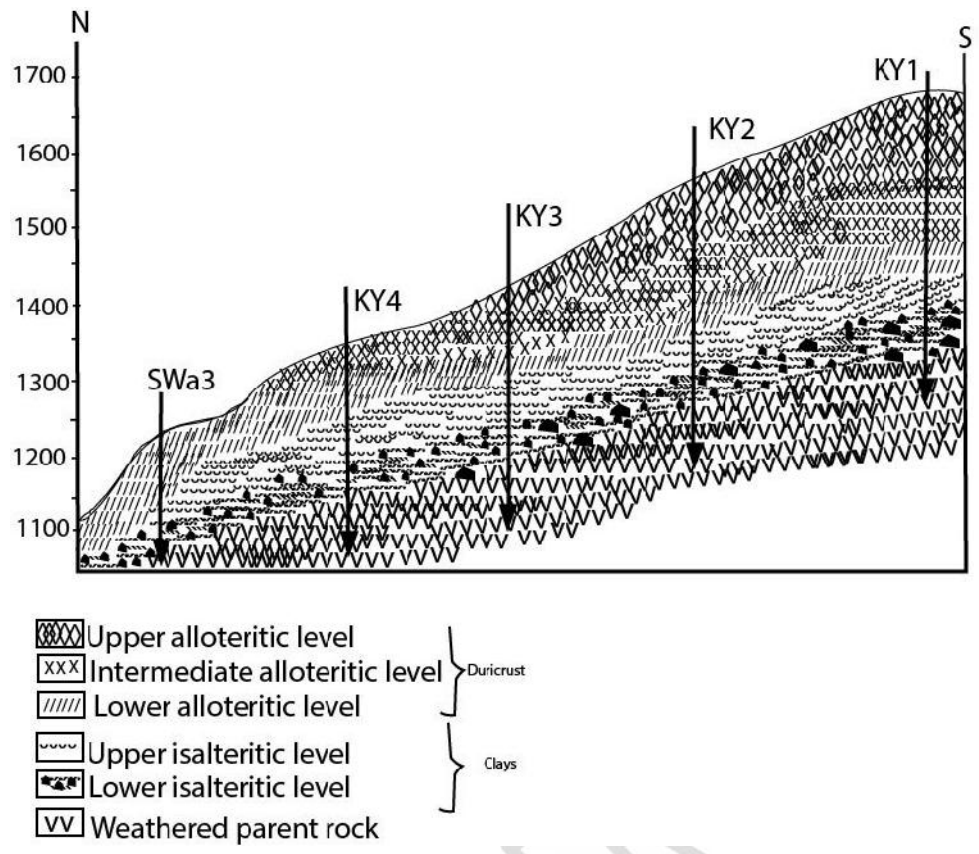


Fig. 2. Toposequence on the flank of Kong-Yeni plateau (Bangam)

UNDER PEE

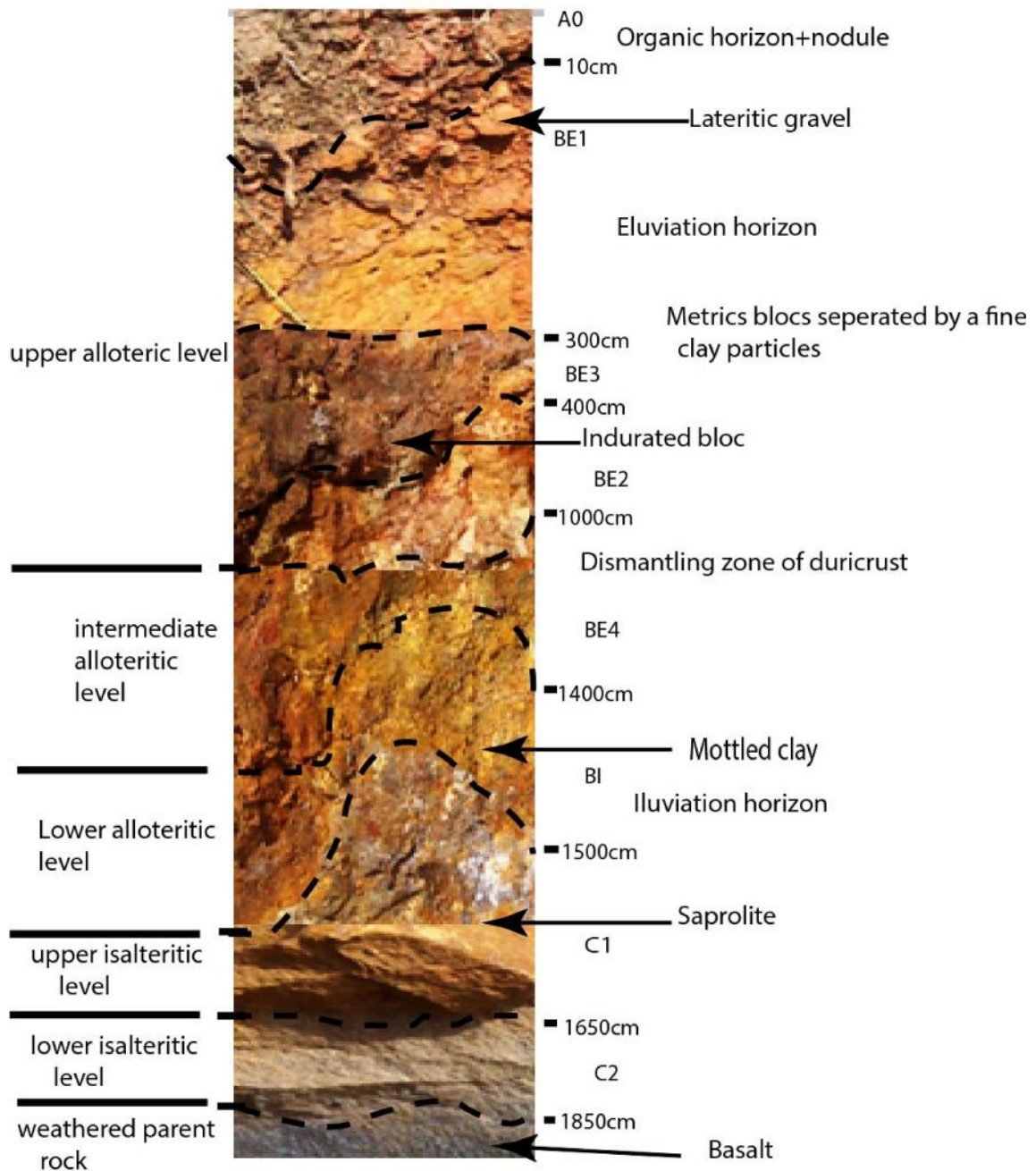
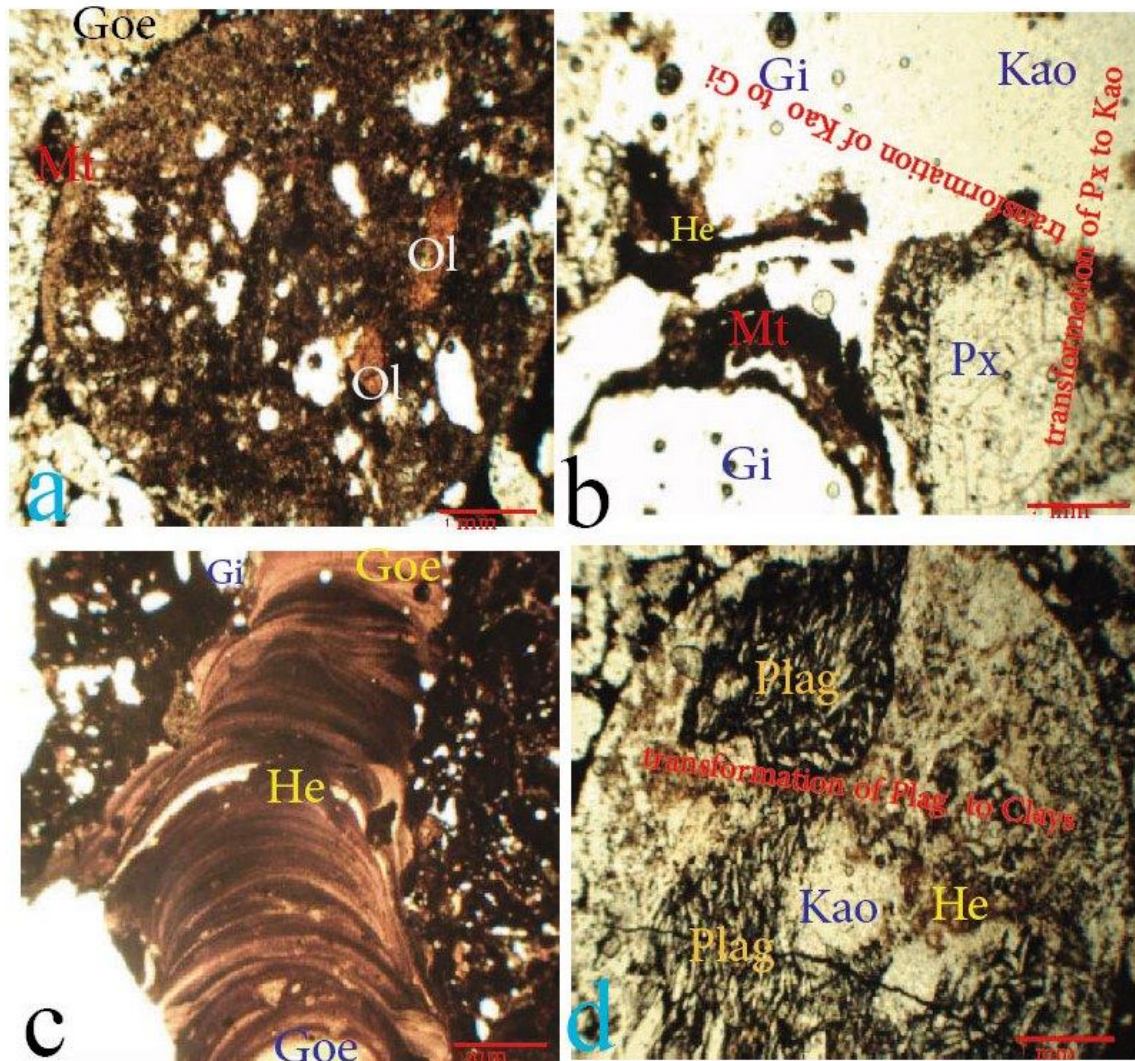


Fig. 3. Overview of weathering mantle



Plag = plagioclases Kao = Kaolinite Gi = gibbsite
 Ol = olivine Goe = goethite Px = pyroxene
 He = hematite Mt = magnetite

Fig. 4. Petrographical observation in thin section.

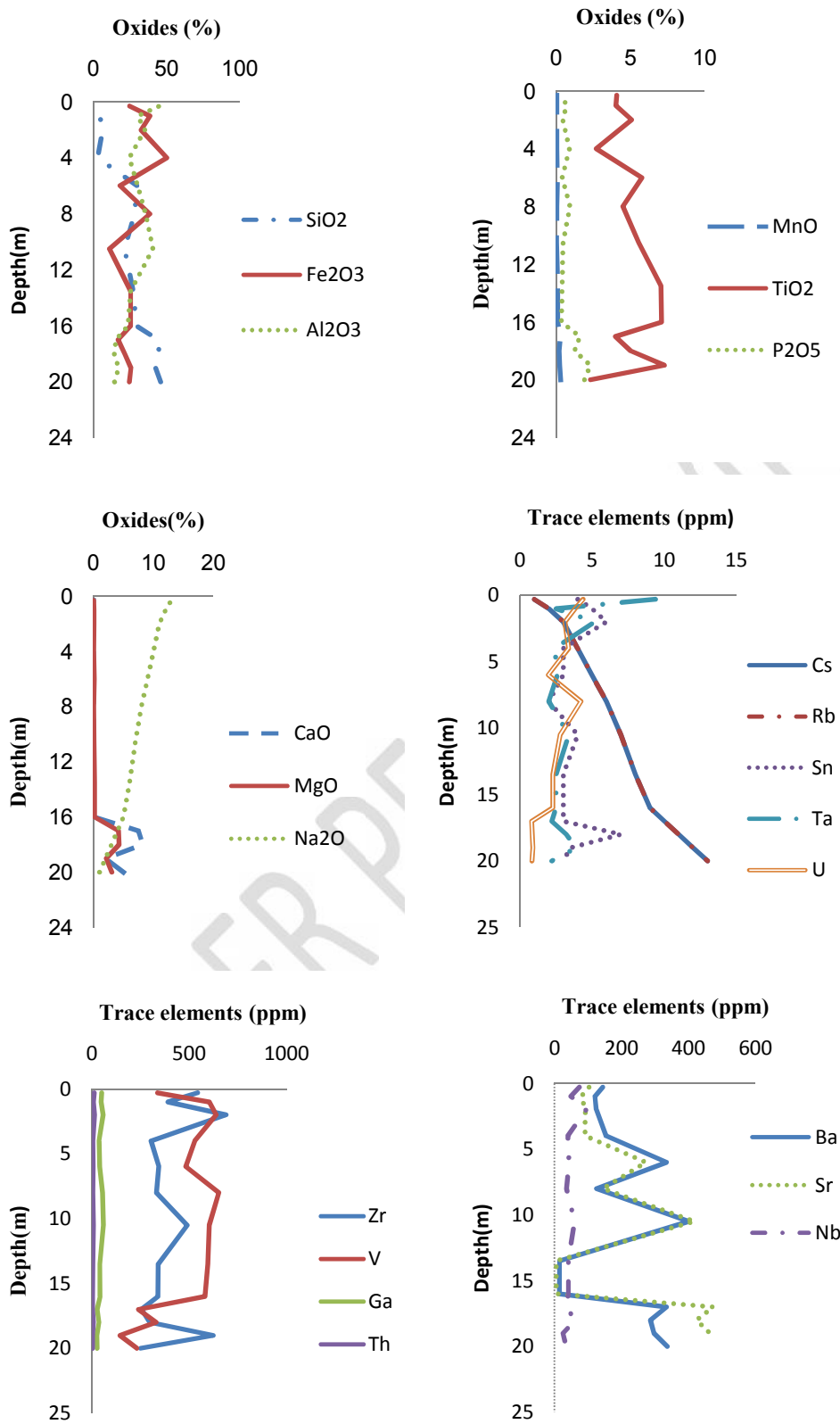
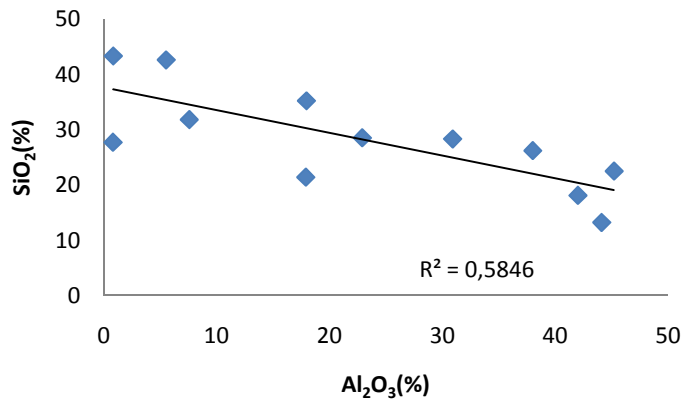
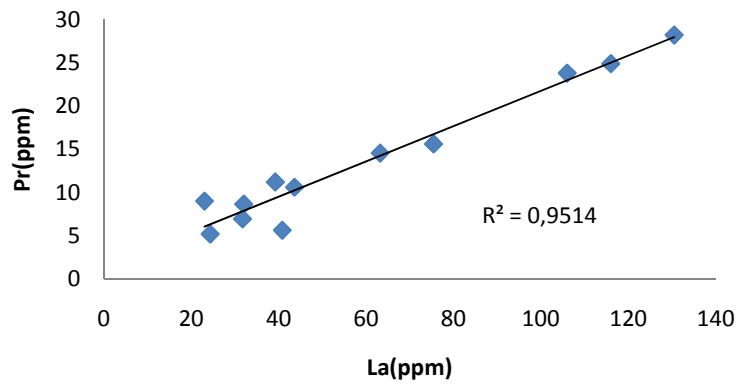


Fig. 5. Chemical elements distribution in the lateritic profile. Concentrations are given as wt% oxide for major elements and ppm for trace elements.



UNDER PEER REVIEW

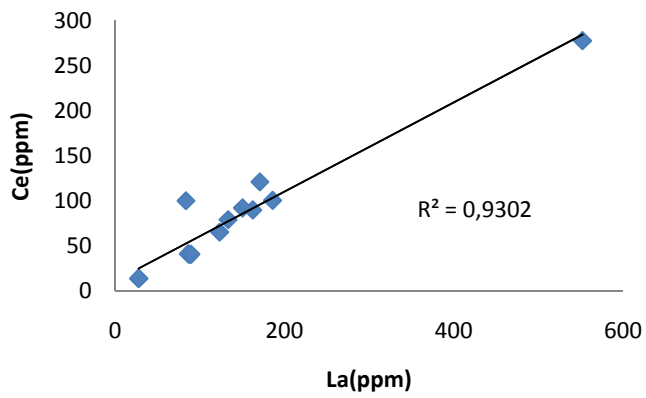
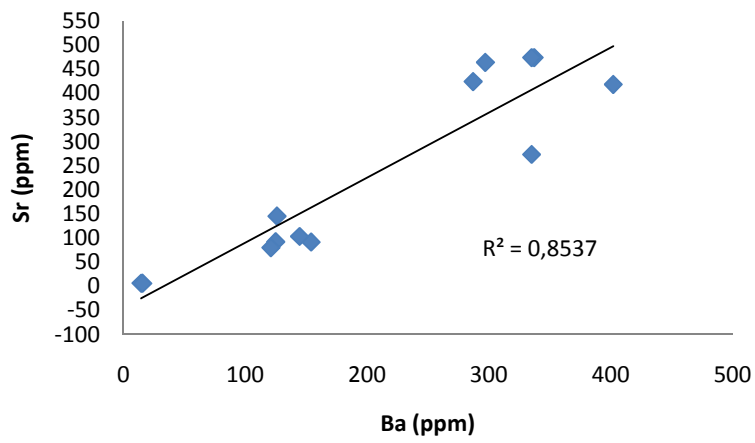


Fig. 6. Binary plots of selected major elements (wt%) and trace and REE elements (ppm) R= Correlation.

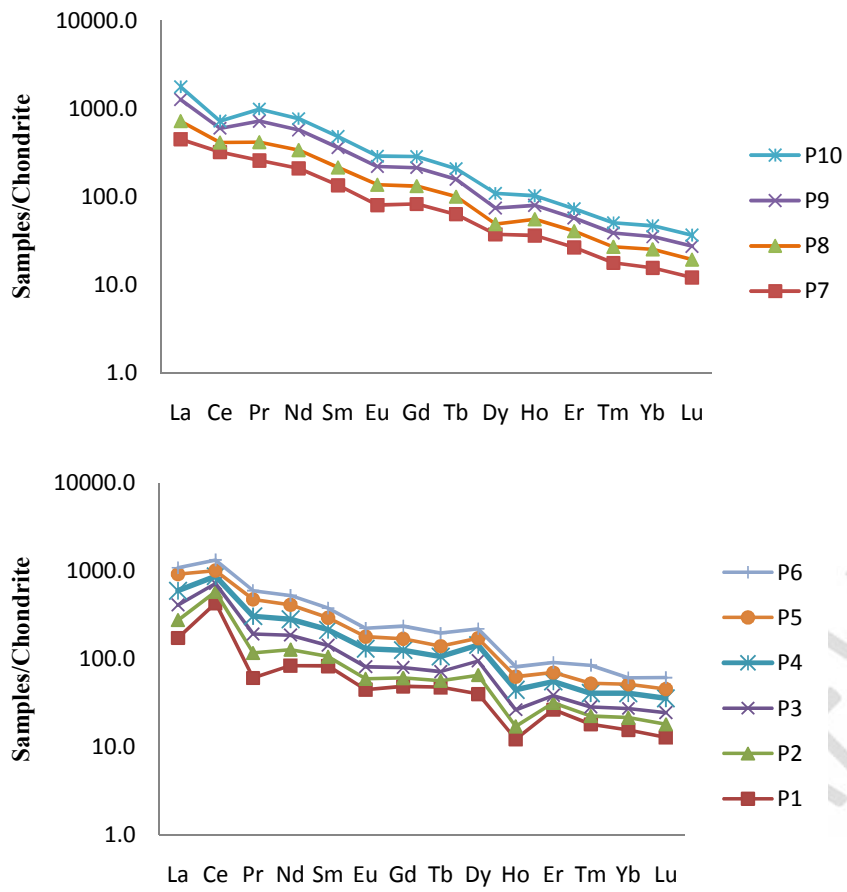


Fig. 7a. Samples/ Chondrite-normalized REE patterns in the weathering KY1 profile

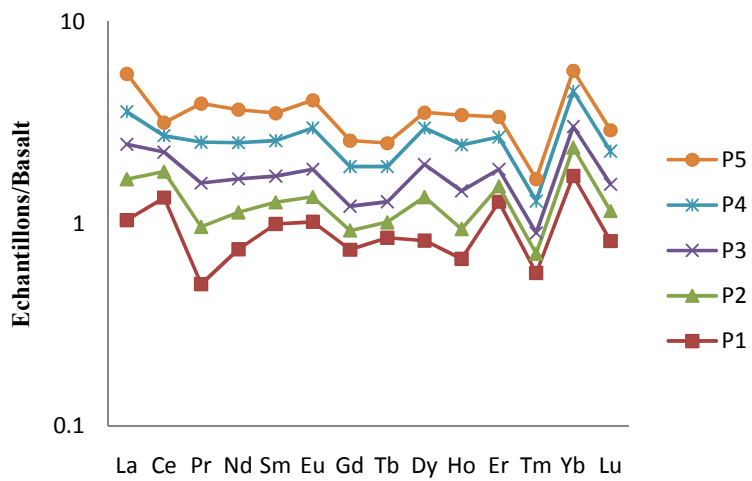
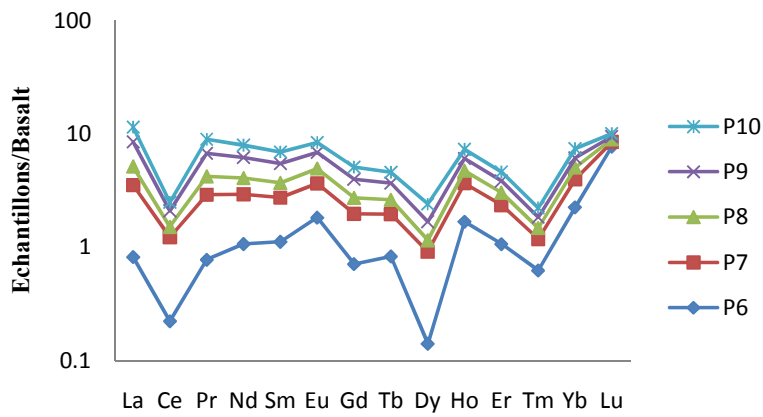


Fig.7b. samples/ Basalt-normalized REE patterns in the weathering profile.

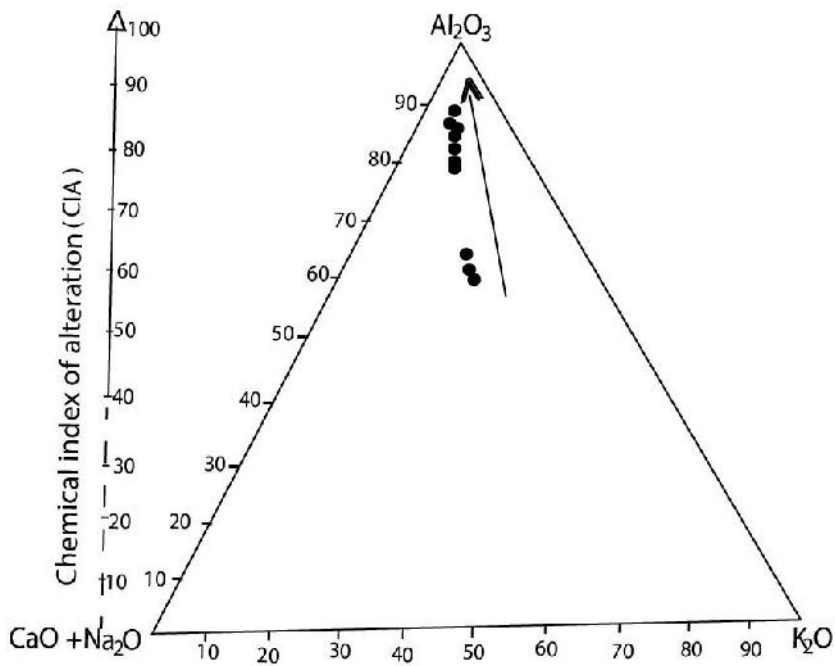


Fig 8a Al_2O_3 - K_2O - $CaO + Na_2O$ (wt%) ternary diagram for the Bangam lateritic profile(KY1).The evolution of feldspars and primary minerals based on Nesbitt and Young (1982).

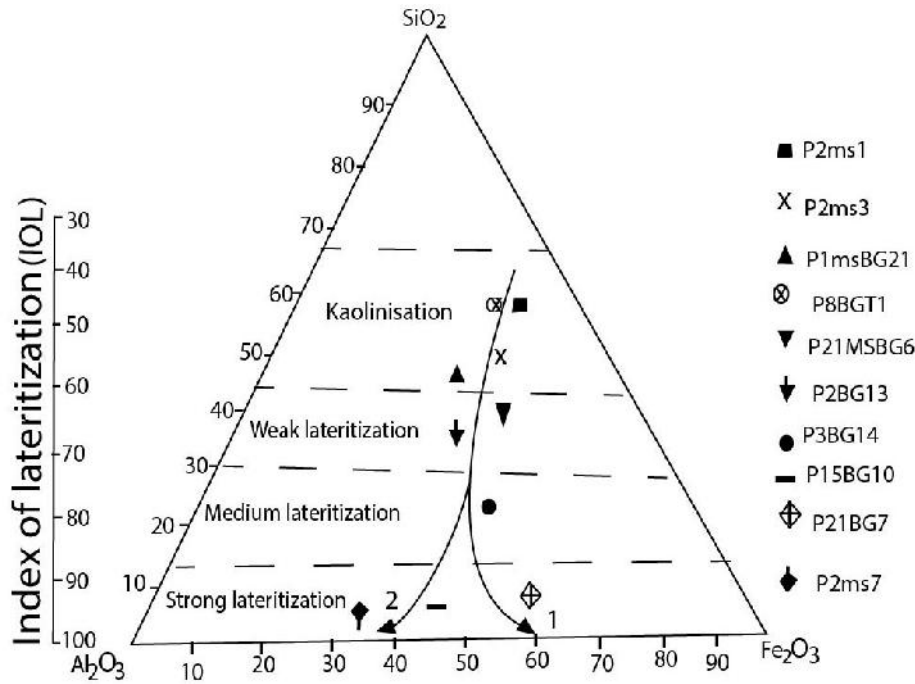


Fig 8b Al_2O_3 - SiO_2 - Fe_2O_3 (wt%) ternary diagram for the Bangam lateritic profile(KY1).The fields of kaolisation, weak, medium and strong lateritization, based on Babechuk et al (2014).